

Linear Flavor-Wave Theory for Fully Antisymmetric $SU(N)$ Irreducible Representations

Francisco H. Kim,¹ Karlo Penc,^{2,3} Pierre Nataf,¹ and Frédéric Mila¹

¹*Institute of Physics, École Polytechnique Fédérale de Lausanne (EPFL), CH-1015 Lausanne, Switzerland*

²*Institute for Solid State Physics and Optics, Wigner Research Centre for Physics,
Hungarian Academy of Sciences, H-1525 Budapest, P.O.B. 49, Hungary*

³*MTA-BME Lendület Magneto-optical Spectroscopy Research Group, 1111 Budapest, Hungary*

(Dated: July 12, 2018)

The extension of the linear flavor-wave theory (LFWT) to fully antisymmetric irreducible representations (irreps) of $SU(N)$ is presented in order to investigate the color order of $SU(N)$ antiferromagnetic Heisenberg models in several two-dimensional geometries. The square, triangular and honeycomb lattices are considered with m fermionic particles per site. We present two different methods: the first method is the generalization of the multiboson spin-wave approach to $SU(N)$ which consists of associating a Schwinger boson to each state on a site. The second method adopts the Read and Sachdev bosons which are an extension of the Schwinger bosons that introduces one boson for each color and each line of the Young tableau. The two methods yield the same dispersing modes, a good indication that they properly capture the semi-classical fluctuations, but the first one leads to spurious flat modes of finite frequency not present in the second one. Both methods lead to the same physical conclusions otherwise: long-range Néel-type order is likely for the square lattice for $SU(4)$ with two particles per site, but quantum fluctuations probably destroy order for more than two particles per site, with $N = 2m$. By contrast, quantum fluctuations always lead to corrections larger than the classical order parameter for the tripartite triangular lattice (with $N = 3m$) or the bipartite honeycomb lattice (with $N = 2m$) for more than one particle per site, $m > 1$, making the presence of color very unlikely except maybe for $m = 2$ on the honeycomb lattice, for which the correction is only marginally larger than the classical order parameter.

I. INTRODUCTION

The experimental research with ultra-cold atomic gases in optical lattices is currently a very active and rapidly progressing field. This type of experiments offers the possibility of fully controlling many parameters, allowing the realization of a vast number of lattice models at low-temperature. It is thus an important tool to help understand the many-body physics of quantum nature. In addition to the well-studied systems with $SU(2)$ symmetry, recent experiments demonstrate that systems characterized by $SU(N)$ with $N \leq 10$ can be implemented with up to two particles per site $m \leq 2$ thanks to the strong decoupling between the electronic angular momentum and the nuclear spin of alkaline-earth atoms.¹⁻³ The high symmetry of $SU(N)$ offers many exciting prospects, such as simulating non-Abelian lattice gauge theories well-known in high-energy physics or implementing quantum computing schemes. Another aspect of interest is the abundance of exotic phases that $SU(N)$ spin Hamiltonian can accommodate.

A simple model that describes the above experimental realization is the fermionic $SU(N)$ Hubbard model

$$\mathcal{H} = -t \sum_{\langle i,j \rangle, \mu} \left(c_{i,\mu}^\dagger c_{j,\mu} + \text{H.c.} \right) + U \sum_{i,\mu < \nu} n_{i,\mu} n_{i,\nu}, \quad (1)$$

where $c_{i,\mu}^\dagger$, $c_{i,\mu}$ are fermionic operators with N flavors μ acting on site i , thus generalizing the conventional two flavor spin Hubbard model to N flavors. In the Mott-insulating phase $t \ll U$ with one particle per site

($m = 1$), we obtain the $SU(N)$ antiferromagnetic (AFM) Heisenberg model

$$\mathcal{H} = J \sum_{\langle i,j \rangle} \sum_{\mu,\nu} \hat{S}_\nu^\mu(i) \hat{S}_\mu^\nu(j), \quad (2)$$

and the operators \hat{S}_ν^μ admit a fermionic representation,

$$\hat{S}_\nu^\mu = f_\nu^\dagger f_\mu - \frac{m}{N} \delta_\nu^\mu. \quad (3)$$

This model has been studied in various settings. A Bethe ansatz solution is known in one dimension for any N ,⁴ along with quantum Monte Carlo (QMC) simulation results.⁵⁻⁷ The investigation of higher dimensional systems often relies on many different numerical techniques. The exact diagonalization^{8,9} can be used for finite cluster sizes, whereas Quantum Monte Carlo methods¹⁰⁻¹⁴ can be applied to problems that do not suffer from the sign problem. The variational Monte Carlo¹⁵⁻¹⁹ and tensor network algorithms²⁰⁻²² have also been employed for $SU(N)$ systems, yielding remarkably accurate results. Analytical investigations have also been carried out, notably using field-theoretical methods in the large- N limit.²³ In particular, chiral spin liquid and valence cluster states are predicted for large N depending on the ratio^{24,25}

$$k = \frac{N}{m}. \quad (4)$$

For small values of N , however, it was shown using the linear flavor-wave theory (LFWT) and different numerical methods that the antiferromagnetically ordered phase

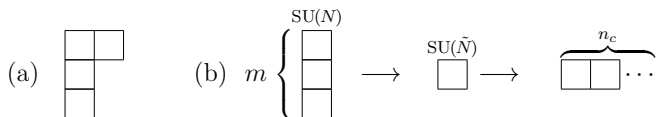


FIG. 1. (a) A generic Young tableau labeled by $[1,0,1]$ or $(2,1,1)$, a partition of $N = 4$. This represents one of the irreducible representations of $SU(4)$. (b) A Young tableau with m vertical boxes representing the corresponding $SU(N)$ irrep with $\tilde{N} = \binom{N}{m}$ states. These states are mapped to states in $SU(\tilde{N})$ fundamental irrep, after which the semi-classical approximation $n_c \rightarrow \infty$ is performed.

is stabilized^{9,20,26,27} for $m = 1$, in which two different colors occupy the adjacent sites of each bond, similar to the spin- $\frac{1}{2}$ Heisenberg square lattice in a Néel configuration. The LFWT, which originates from the pioneering works of Papanicolaou^{28,29} and which was further developed by Joshi *et al.*³⁰ and Chubukov³¹, assesses the possibility of a system to retain a long-range order with quantum fluctuations, and it predicts a magnetic order for $m = 1$ up to $N = 5$ for the square lattice, and for $N = 3$ for the triangular lattice.^{32,33} It is expected that the magnetic order would be destroyed as k becomes large due to the increase of quantum fluctuations and the frustration in the system that stems from the extensively degenerate ground-state manifold at the mean-field level for large N . So far, the LFWT has been applied uniquely on the systems with one particle per site ($m = 1$), and it is not yet known if the magnetic order would survive in systems with relatively small k and m with more than one particle per site ($m > 1$).

When placing one particle per site, the N degrees of freedom of $SU(N)$, called colors or flavors in reference to elementary particles, lead to the use of the fundamental irreducible representation of $SU(N)$, in which the $SU(N)$ matrices act on the N -dimensional complex-vector space. However, placing many particles per site can be seen as generating new composite particles (e.g., quarks giving mesons in particle physics), and the action of $SU(N)$ has to be adapted to the composite particles, meaning that a different irreducible representation (irrep) of $SU(N)$ has to be considered. An irreducible representation of $SU(N)$ can be depicted by a Young tableau, labeled by the row lengths (l_1, \dots, l_k) or, alternatively, labeled by a $(N-1)$ -tuple whose entry is the difference of the length of the adjacent rows $[l_1 - l_2, l_2 - l_3, \dots, l_k - 0]$. The antisymmetry of the states is represented in the vertically stacked boxes, whereas the symmetry is represented in the horizontally stacked boxes, leading to the constraint that a Young tableau cannot have more than N rows ($1 \leq k \leq N$). Additionally, a row cannot be longer than the row above it ($l_k \leq \dots \leq l_1$).

In this work, we present two different methods of applying the LFWT to arbitrary irreducible representations, with emphasis on fully antisymmetric irreps. Such irreps, with a single column of length m , are very natural in the context of fermionic cold atoms in optical lattices

because they describe the Mott phases with m particles per site. Owing to the strong hyperfine interactions, it is possible to load fermionic atoms with an internal degree of freedom that can take up to N values, thus implementing the $SU(N)$ symmetry. It is then possible to load up to N particles per site, and if the on-site repulsion is strong enough, to stabilize Mott phases with m particles per site for $1 \leq m \leq N$. The best candidates are ytterbium, for which N can be as large as 6, and strontium, for which N can be as large as 10.

The first method is an extension of the multiboson spin-wave^{34–36} to $SU(N)$ irreps, where each state of a given irrep is represented by a boson. A second approach relies on a different bosonic representation of the states of a given $SU(N)$ antisymmetric irrep, used by Read and Sachdev.²³ Based on the ordered nature of the ground-state we are considering, we assume a condensate of multiple colors on each sublattice, enabling the c -number substitution of the condensed bosons in the spirit of Bogoliubov.³⁷ Both procedures are applied to all the simplest two-dimensional geometries that can accommodate an antiferromagnetic color order without frustration. When the classical ground-state manifold is infinitely degenerate as in the $SU(3)$ AFM Heisenberg model on the square lattice, the LFWT cannot give an accurate prediction of the color order due to the infrared divergency stemming from the degenerate classical ground-states, although this degeneracy is expected to be lifted by quantum fluctuations, thus allowing the system to retain a small color order (see Ref. 38).

Henceforth, we consider the square lattice and the honeycomb lattice in a Néel-like two-sublattice configuration ($n_{\text{sub}} = 2$), and the triangular lattice with three sublattices ($n_{\text{sub}} = 3$), with n_{sub} being the number of sublattices required for a frustration-free color-order. For an antiferromagnetic Heisenberg model with a given N , it is then natural to consider $m = \frac{N}{n_{\text{sub}}}$ particles per site. We thus apply the method to the $SU(4)$ AFM Heisenberg model with $m = 2$ on the bipartite square lattice and on the bipartite honeycomb lattice, and we continue with the $SU(6)$ AFM Heisenberg model with $m = 2$ on the tripartite triangular lattice. We then derive results for any N on these geometries. We show that $N = 4$ on the bipartite square lattice is the only case that can possess long-range order, in other cases the zero-point quantum fluctuations will destroy the order.

II. MULTIBOSON LFWT APPROACH

We hereby address fully antisymmetric states expressed in terms of m fermions per site. The Young tableau of the corresponding irrep then consists of a single column with m boxes. In the fundamental representation, the fermionic representation Eq. (3) allows us to

write the Heisenberg Hamiltonian, Eq. (2), as

$$\mathcal{H} = J \sum_{\langle i,j \rangle} \sum_{\mu,\nu=1}^N f_{\nu,i}^\dagger f_{\mu,i} f_{\mu,j}^\dagger f_{\nu,j}, \quad (5)$$

where the constant term $-\frac{m^2}{N}$ has been dropped. The Hamiltonian is then simply a permutation of two colors from two neighboring sites. m fermionic particles in an antisymmetric configuration form

$$\tilde{N} := \binom{N}{m} \quad (6)$$

states on a site that transform into themselves according to the corresponding irrep. We can thus assign a boson to each state of the irrep, providing \tilde{N} bosons, and we can rewrite the action of the Hamiltonian (i.e., the color permutation) in the basis of this irrep. This amounts to mapping our original states to $SU(\tilde{N})$ states in the fundamental irrep. The boson that represents the classical ground state can then be condensed in order to perform the semi-classical expansion by letting $n_c \rightarrow \infty$ (see Fig. 1). This is analog to the spin-wave expansion where we let $S \rightarrow \infty$. The value of n_c will be set to 1 at the end of the calculations.

A. $SU(4)$ $m = 2$ on the square lattice

Let us first consider $SU(4)$ with $m = 2$ on a bipartite square lattice, on which we assume a Néel-like two-sublattice ordered state (see Fig. 2). Furthermore, we assume that the first two colors A and B are condensed on sublattice Γ_{AB} and the last two colors on sublattice Γ_{CD} . The irrep we are considering is thus $[0, 1, 0]$. Let the basis of this six-dimensional irrep be

$$\left\{ \frac{1}{\sqrt{2}} (|AB\rangle - |BA\rangle), \frac{1}{\sqrt{2}} (|AC\rangle - |CA\rangle), \frac{1}{\sqrt{2}} (|DA\rangle - |AD\rangle), \frac{1}{\sqrt{2}} (|BC\rangle - |CB\rangle), \frac{1}{\sqrt{2}} (|BD\rangle - |DB\rangle), \frac{1}{\sqrt{2}} (|CD\rangle - |DC\rangle) \right\}, \quad (7)$$

which we label conveniently as the elements of the set

$$S := \{AB, AC, DA, BC, BD, CD\}. \quad (8)$$

Note that a different choice of basis does not affect the spectra of the Hamiltonian at the end of the calculations. It is also worthwhile noting that an orthogonal basis can be systematically found for any irrep of $SU(N)$ by using the orthogonal units developed by Young.⁹ This yields six Schwinger bosons $b_{AB}^\dagger, b_{AC}^\dagger, b_{DA}^\dagger, b_{BC}^\dagger, b_{BD}^\dagger, b_{CD}^\dagger$ and their Hermitian counterparts in this basis of the irrep, and they describe the composite particles composed of

two $SU(4)$ color particles. The generators for a given site i can be written as

$$\hat{S}_\nu^\mu(i) = \sum_{\substack{\alpha=A \\ \alpha \neq \mu, \nu}}^D b_{\alpha\nu}^\dagger(i) b_{\alpha\mu}(i), \quad (9)$$

in which the bosons are antisymmetric in their indices, $b_{\nu\mu}^\dagger = -b_{\mu\nu}^\dagger$, such that the indices can be ordered to yield the aforementioned labels $\{AB, AC, DA, BC, BD, CD\}$. The sign of the permutations takes into account the antisymmetry of the resulting states. As an example, the operator \hat{S}_C^A is given as

$$\hat{S}_C^A(i) = -b_{BC}^\dagger(i) b_{AB}(i) - b_{CD}^\dagger(i) b_{DA}(i), \quad (10)$$

which is exchanging color A with color C in all the states that allow this transition. The diagonal operator \hat{S}_C^C would be given as

$$\hat{S}_C^C(i) = b_{AC}^\dagger(i) b_{AC}(i) + b_{BC}^\dagger(i) b_{BC}(i) + b_{CD}^\dagger(i) b_{CD}(i). \quad (11)$$

This representation of the $SU(N)$ generators \hat{S}_ν^μ satisfies the $SU(N)$ commutation relation

$$[\hat{S}_\beta^\alpha, \hat{S}_\nu^\mu] = \delta_\nu^\alpha \hat{S}_\beta^\mu - \delta_\beta^\mu \hat{S}_\nu^\alpha. \quad (12)$$

The Hamiltonian (2) can then be written in terms of the Schwinger bosons. This result is obtained by writing the Hamiltonian Eq. (5) in the basis of the two-site Hilbert space.

In the language of the composite particles, the constraint $m = 2$ can be written as

$$\sum_\eta b_\eta^\dagger(i) b_\eta(i) = n_c, \quad (13)$$

where $n_c = 1$ and $\eta \in S$.

Let the site $i_{AB} \in \Gamma_{AB}$ and the site $i_{CD} \in \Gamma_{CD}$. It is now possible to apply the standard linear flavor-wave theory as in Ref. 38. Similar to the $1/S$ expansion in the spin-wave theory, the limit $n_c \rightarrow \infty$ allows us to write

$$\begin{aligned} b_\lambda^{\lambda\dagger}(i_\lambda) b_\lambda^\lambda(i_\lambda) &= n_c - \sum_{\eta \in S \setminus \{\lambda\}} b_\eta^{\lambda\dagger}(i_\lambda) b_\eta^\lambda(i_\lambda) \\ \Rightarrow b_\lambda^{\lambda\dagger}(i_\lambda), b_\lambda^\lambda(i_\lambda) &\rightarrow \sqrt{n_c - \sum_{\eta \in S \setminus \{\lambda\}} b_\eta^{\lambda\dagger}(i_\lambda) b_\eta^\lambda(i_\lambda)} \end{aligned} \quad (14)$$

where the superscript $\lambda \in L := \{AB, CD\}$ refers to the corresponding sublattice in the spirit of the Holstein-Primakoff representation. Expanding the square roots in $1/n_c$ gives rise to a decomposition of the Hamiltonian in powers of $\sqrt{n_c}$:

$$\mathcal{H} = \mathcal{H}^{(0)} + \mathcal{H}^{(1)} + \mathcal{H}^{(2)} + \mathcal{O}(n_c^{-\frac{1}{2}}). \quad (15)$$

The term $\mathcal{H}^{(0)} \propto n_c^2$ is the classical energy, whereas $\mathcal{H}^{(1)} \propto n_c^{\frac{3}{2}}$ is the linear term that vanishes if we start

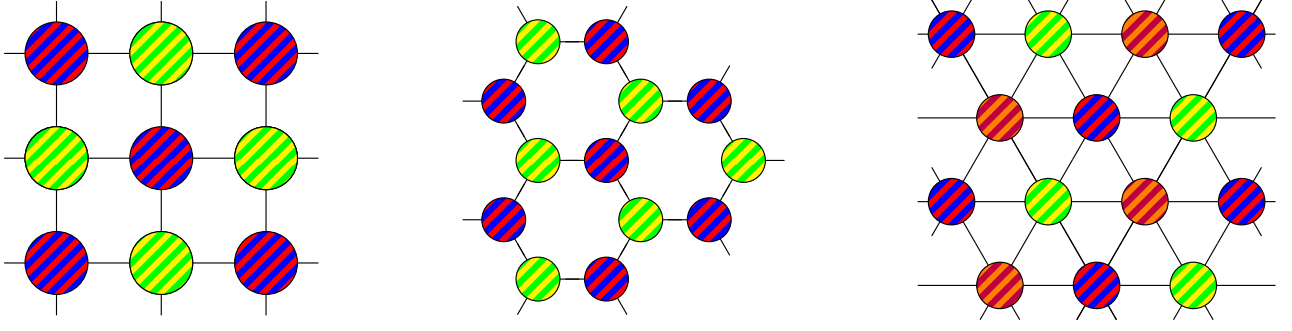


FIG. 2. A Néel-like two-sublattice order on the square lattice and the honeycomb lattice with two particles per site for the SU(4) AFM Heisenberg model, and a three-sublattice order on the triangular lattice with two particles per site for SU(6).

from a classical ground state. In the following, we truncate the Hamiltonian at the harmonic order and consider the quadratic term $\mathcal{H}^{(2)}$ only. After the Fourier transform

$$b_\eta^\lambda(i_\lambda) = \sqrt{\frac{2}{N}} \sum_{\mathbf{k} \in \text{RBZ}} b_\eta^\lambda(\mathbf{k}) e^{-i\mathbf{k} \cdot \mathbf{x}_i}, \quad (16)$$

the quadratic Hamiltonian is given by

$$\begin{aligned} \mathcal{H}^{(2)} = Jn_c \sum_{\mathbf{k} \in \text{RBZ}} & \left[8b_{CD}^{AB\dagger}(\mathbf{k}) b_{CD}^{AB}(\mathbf{k}) + 8b_{AB}^{CD\dagger}(\mathbf{k}) b_{AB}^{CD}(\mathbf{k}) \right. \\ & + 4\gamma_{\text{sq}}(\mathbf{k}) b_{AC}^{AB\dagger}(\mathbf{k}) b_{BD}^{CD\dagger}(-\mathbf{k}) + 4\gamma_{\text{sq}}(\mathbf{k}) b_{AC}^{AB}(\mathbf{k}) b_{BD}^{CD}(-\mathbf{k}) + 4b_{AC}^{AB\dagger}(\mathbf{k}) b_{AC}^{AB}(\mathbf{k}) + 4b_{BD}^{CD\dagger}(-\mathbf{k}) b_{BD}^{CD}(-\mathbf{k}) \\ & + 4\gamma_{\text{sq}}(\mathbf{k}) b_{BD}^{AB\dagger}(\mathbf{k}) b_{AC}^{CD\dagger}(-\mathbf{k}) + 4\gamma_{\text{sq}}(\mathbf{k}) b_{BD}^{AB}(\mathbf{k}) b_{AC}^{CD}(-\mathbf{k}) + 4b_{BD}^{AB\dagger}(\mathbf{k}) b_{BD}^{AB}(\mathbf{k}) + 4b_{AC}^{CD\dagger}(-\mathbf{k}) b_{AC}^{CD}(-\mathbf{k}) \\ & + 4\gamma_{\text{sq}}(\mathbf{k}) b_{DA}^{AB\dagger}(\mathbf{k}) b_{BC}^{CD\dagger}(-\mathbf{k}) + 4\gamma_{\text{sq}}(\mathbf{k}) b_{DA}^{AB}(\mathbf{k}) b_{BC}^{CD}(-\mathbf{k}) + 4b_{DA}^{AB\dagger}(\mathbf{k}) b_{DA}^{AB}(\mathbf{k}) + 4b_{BC}^{CD\dagger}(-\mathbf{k}) b_{BC}^{CD}(-\mathbf{k}) \\ & \left. + 4\gamma_{\text{sq}}(\mathbf{k}) b_{BC}^{AB\dagger}(\mathbf{k}) b_{DA}^{CD\dagger}(-\mathbf{k}) + 4\gamma_{\text{sq}}(\mathbf{k}) b_{BC}^{AB}(\mathbf{k}) b_{DA}^{CD}(-\mathbf{k}) + 4b_{BC}^{AB\dagger}(\mathbf{k}) b_{BC}^{AB}(\mathbf{k}) + 4b_{DA}^{CD\dagger}(-\mathbf{k}) b_{DA}^{CD}(-\mathbf{k}) \right], \end{aligned} \quad (17)$$

with

$$\gamma_{\text{sq}}(\mathbf{k}) = \frac{1}{2}(\cos k_x + \cos k_y), \quad (18)$$

After the diagonalization of the non-diagonal terms (the only diagonal terms being those with b_{CD}^{AB} and b_{AB}^{CD}) with the help of an adequate Bogoliubov transformation,

$$\begin{pmatrix} \tilde{b}_{AC,\mathbf{k}}^{AB\dagger} \\ \tilde{b}_{BD,-\mathbf{k}}^{CD} \end{pmatrix} = \begin{pmatrix} u_{\mathbf{k}} & v_{\mathbf{k}} \\ v_{\mathbf{k}} & u_{\mathbf{k}} \end{pmatrix} \begin{pmatrix} b_{AC,\mathbf{k}}^{AB\dagger} \\ b_{BD,-\mathbf{k}}^{CD} \end{pmatrix} \quad (19)$$

and similarly for other bosons, the resulting harmonic Hamiltonian reads as

$$\begin{aligned} \mathcal{H}^{(2)} = Jn_c \sum_{\mathbf{k} \in \text{RBZ}} & \left[8 \left(b_{CD}^{AB\dagger}(\mathbf{k}) b_{CD}^{AB}(\mathbf{k}) + b_{AB}^{CD\dagger}(\mathbf{k}) b_{AB}^{CD}(\mathbf{k}) \right) \right. \\ & \left. + \omega_{\text{sq}}(\mathbf{k}) \sum_{\lambda \in L} \sum_{\eta \in S \setminus L} \left(\tilde{b}_\eta^{\lambda\dagger}(\mathbf{k}) \tilde{b}_\eta^\lambda(\mathbf{k}) + \frac{1}{2} \right) \right] \\ & - 16Jn_c \frac{N}{2}, \end{aligned} \quad (20)$$

with

$$\omega_{\text{sq}}(\mathbf{k}) = 4\sqrt{1 - |\gamma_{\text{sq}}(\mathbf{k})|^2}. \quad (21)$$

The dispersion relation is depicted in Fig. 3. Note that it is identical to the dispersion relation of SU(2).

Alternatively, in the structural Brillouin zone, we obtain

$$\begin{aligned} \mathcal{H}^{(2)} = Jn_c \sum_{\mathbf{k}} & \left\{ 8b^\dagger(\mathbf{k}) b(\mathbf{k}) \right. \\ & \left. + \omega_{\text{sq}}(\mathbf{k}) \sum_{\beta=1}^4 \left(\tilde{b}_\beta^\dagger(\mathbf{k}) \tilde{b}_\beta(\mathbf{k}) + \frac{1}{2} \right) \right\} - 8Jn_c N, \end{aligned} \quad (22)$$

in which the boson b^\dagger originates from the decoupled bosons b_{CD}^{AB} and b_{CD}^{AB} , whereas the bosons \tilde{b}^\dagger stem from the Bogoliubov transformation in Eq. (19). We obtain 10 bands in the reduced Brillouin zone, which correspond to 5 bands in the structural Brillouin zone. From the 5 branches, four are dispersive and one is flat at energy $8Jn_c$. The (degenerate) dispersive bands are associated to the possible flavour-exchanges (e.g., $A \leftrightarrow C$

and $A \leftrightarrow D$). The flat band, however, originates from having the same colors AB (or CD) on two neighboring sites of a bond. This is a higher-order transition, as two colors are different with respect to the chosen classical ground-state. In other words, it requires the action of two ladder operators: this can be seen in the weight diagram of this irrep, Fig. 4, where AB and CD are two edges apart. Thus this higher-order excitation does not interact in the harmonic order of the bilinear Heisenberg exchange Hamiltonian,³⁵ and this results in a localized flat band.

The energy per site of the system due to quantum fluctuations is

$$\begin{aligned} E/N &= Jn_c \left(-8 + 4 \cdot \left\langle \frac{\omega_{\text{sq}}(\mathbf{k})}{2} \right\rangle \right) \\ &= -1.264Jn_c. \end{aligned} \quad (23)$$

We now define the ordered color moment on the site $i \in \Gamma_\lambda$, as

$$\begin{aligned} m_i &= \frac{1}{n_c} \left\langle b_\lambda^{\lambda\dagger}(i)b_\lambda^\lambda(i) \right\rangle \\ &= \frac{1}{n_c} \left(n_c - \left\langle \sum_{\eta \in S \setminus \{\lambda\}} b_\eta^{\lambda\dagger}(i)b_\eta^\lambda(i) \right\rangle \right), \end{aligned} \quad (24)$$

so that the fully polarized classical Néel state is $m_i = 1$. Then, the reduction of the ordered moment due to quantum fluctuations is

$$\begin{aligned} \Delta m_i &= \frac{1}{n_c} \left\langle \sum_{\eta \in S \setminus \{\lambda\}} b_\eta^{\lambda\dagger}(i)b_\eta^\lambda(i) \right\rangle \\ &= \left\langle 4 \cdot \frac{1}{2} \left(\frac{4Jn_c}{Jn_c\omega_{\text{sq}}} - 1 \right) \right\rangle \\ &= 0.786, \end{aligned} \quad (25)$$

where we used the fact that $\langle b_{CD}^{AB\dagger}(i)b_{CD}^{AB}(i) \rangle = \langle b_{AB}^{CD\dagger}(i)b_{AB}^{CD}(i) \rangle = 0$ whereas $\langle b_\eta^{\lambda\dagger}(i)b_\eta^\lambda(i) \rangle$ is finite for $\lambda \in L$ and $\eta \in S \setminus \{\lambda\}$ as a consequence of the Bogoliubov transformation. This merely reflects the impossibility for the state AB to fluctuate into the state CD with the bilinear Heisenberg exchange in the harmonic order.

The ordered moment is then

$$m_i = 1 - \Delta m_i = 0.214. \quad (26)$$

Since the ordered moment $m_i > 0$, this theory predicts that the system potentially retains a finite magnetic order. Note that the correction is not small, however. It is close to 80%. So, order is likely but not guaranteed.

Note that we could alternatively define the ordered moment as in Ref. 14 in which it is defined on any site i of a bipartite lattice as

$$m_i^{\text{alt}} = \frac{2}{N} \left(\sum_{\mu=1}^{N/2} S_\mu^\mu(i) - \sum_{\mu=\frac{N}{2}+1}^N S_\mu^\mu(i) \right), \quad (27)$$

giving an ordered moment of $m_i = (-1)^i$ for a classical Néel configuration, where the sign depends on the sublattice. Following this definition, one finds

$$m_i^{\text{alt}} = (-1)^i 0.214. \quad (28)$$

B. $SU(4)$ $m = 2$ on the honeycomb lattice

Following the same construction as in Sec. II A, we assume two sublattices Γ_{AB} and Γ_{CD} , and $L = \{AB, CD\}$, $S = \{AB, AC, DA, BC, BD, CD\}$ as before (see Fig. 2). Then the harmonic Hamiltonian for the bipartite honeycomb lattice can be given as follows:

$$\begin{aligned} \mathcal{H}^{(2)} &= Jn_c \sum_{\mathbf{k} \in \text{BZ}} \left[6 \sum_{\lambda \in L} \sum_{\eta \in L \setminus \{\lambda\}} b_\eta^{\lambda\dagger}(\mathbf{k})b_\eta^\lambda(\mathbf{k}) \right. \\ &\quad \left. + \omega_{\text{hon}}(\mathbf{k}) \sum_{\lambda \in L} \sum_{\eta \in S \setminus L} \left(\tilde{b}_\eta^{\lambda\dagger}(\mathbf{k})\tilde{b}_\eta^\lambda(\mathbf{k}) + \frac{1}{2} \right) \right] - 6Jn_c N, \end{aligned} \quad (29)$$

where \mathbf{k} run over the structural Brillouin zone of the honeycomb lattice, thus giving rise to doubly degenerate bands. The dispersion relation of the dispersive (“magnetic”) branch (see Fig. 3) is given by

$$\omega_{\text{hon}}(\mathbf{k}) = 3\sqrt{1 - |\gamma_{\text{hon}}(\mathbf{k})|^2}, \quad (30)$$

where

$$\gamma_{\text{hon}}(\mathbf{k}) = \frac{1}{3} \left(e^{ik_y} + e^{i\left(\frac{\sqrt{3}}{2}k_x - \frac{1}{2}k_y\right)} + e^{i\left(-\frac{\sqrt{3}}{2}k_x - \frac{1}{2}k_y\right)} \right). \quad (31)$$

The energy per site due to quantum fluctuations is

$$\begin{aligned} E/N &= Jn_c \left(-6 + 4 \cdot \left\langle \frac{\omega_{\text{hon}}(\mathbf{k})}{2} \right\rangle \right) \\ &= -1.259Jn_c. \end{aligned} \quad (32)$$

The reduction of the ordered moment is

$$\begin{aligned} \Delta m_i &= \frac{1}{n_c} \left\langle \sum_{\eta=2}^6 b_\eta^{1\dagger}(i)b_\eta^1(i) \right\rangle \\ &= \frac{1}{n_c} \left\langle 4 \cdot \frac{1}{2} \left(\frac{4Jn_c}{Jn_c\omega_{\text{hon}}} - 1 \right) \right\rangle \\ &= 1.0328. \end{aligned} \quad (33)$$

The reduction is larger than the classical moment. It is thus likely that no finite order exists on the two-sublattice honeycomb lattice for $N = 4$ with two particles per site. Note, however, that the reduction is only marginally above 100%. So, it cannot be excluded on this basis that a small moment survives quantum fluctuations.

C. SU(6) $m = 2$ on the triangular lattice

Similar considerations can be done for the triangular lattice for which we assume a three-sublattice order with two particles per site, i.e., with sublattices $\Gamma_{AB}, \Gamma_{CD}, \Gamma_{EF}$ where we assume a basis similar to Eq. (7) (see Fig. 2).

Adding all the bonds together and merging them to form bands in the structural Brillouin zone, we obtain

$$\mathcal{H}^{(2)} = Jn_c \sum_{\mathbf{k}} \left[\sum_{\alpha=1}^6 6b_{\alpha}^{\dagger}(\mathbf{k})b_{\alpha}(\mathbf{k}) + \omega_{\text{tri}}(\mathbf{k}) \sum_{\beta=1}^8 \left(\tilde{b}_{\beta}^{\dagger}(\mathbf{k})\tilde{b}_{\beta}(\mathbf{k}) + \frac{1}{2} \right) \right] - 12Jn_c, \quad (34)$$

with the dispersion relation (see Fig. 3)

$$\omega_{\text{tri}}(\mathbf{k}) = 3\sqrt{1 - |\gamma_{\text{tri}}(\mathbf{k})|^2} \quad (35)$$

in which

$$\gamma_{\text{tri}}(\mathbf{k}) = \frac{1}{3} \left(e^{ik_x} + 2e^{-i\frac{1}{2}k_x} \cos \frac{\sqrt{3}}{2}k_y \right). \quad (36)$$

It is worth noting the similarity between Eqs. (36) and (31), as the geometric bonds between two sublattices have the same angle in both the triangular and the honeycomb lattices. We obtain six bands that sit high in energy and eight bands associated to the exchange of flavors that always keep one flavor on the site, e.g., AB to AC .

The energy per site due to quantum fluctuations is

$$\begin{aligned} E/N &= Jn_c \left(-12 + 8 \cdot \left\langle \frac{\omega_{\text{tri}}(\mathbf{k})}{2} \right\rangle \right) \\ &= -2.518Jn_c. \end{aligned} \quad (37)$$

The reduction of the ordered moment is

$$\begin{aligned} \Delta m_i &= \frac{1}{n_c} \left\langle \sum_{\eta=2}^{15} b_{\mu}^{\dagger}(i)b_{\mu}^{\eta}(i) \right\rangle \\ &= \frac{1}{n_c} \left\langle 8 \cdot \frac{1}{2} \left(\frac{3Jn_c}{Jn_c\omega_{\text{tri}}(\mathbf{k})} - 1 \right) \right\rangle \\ &= 2.066, \end{aligned} \quad (38)$$

hence, we can conclude that the long-range color order is almost certainly destroyed by quantum fluctuations.

D. General m

For any antisymmetric $SU(N)$ irrep with m particles, the generators \hat{S}_{ν}^{μ} for a given site i can be written as

$$\begin{aligned} \hat{S}_{\nu}^{\mu}(i) &= \sum_{\substack{\alpha_1, \dots, \alpha_m \\ \alpha_1, \dots, \alpha_m \neq \mu, \nu}} \text{sgn}(\sigma_1) \text{sgn}(\sigma_2) \\ &\quad \times b_{\sigma_1 \cdot (\alpha_1 \dots \alpha_m \nu)}^{\dagger}(i) b_{\sigma_2 \cdot (\alpha_1 \dots \alpha_m \mu)}(i), \end{aligned} \quad (39)$$

with $\alpha_1, \dots, \alpha_m$ run over the N colors and σ_1, σ_2 are permutations that order the letters in the alphabetical order. This is a direct generalization of Eq. (9), and its action is the permutation of color μ with ν while taking care of the sign change due to the antisymmetry of the states. Note that this can be generalized further for any general irrep by determining the action of the generator \hat{S}_{ν}^{μ} on the basis states of the irrep.

From the three models above, we observe the existence of dispersive branches and non-zero flat branches at the harmonic level of the Hamiltonian. The dispersive branches stem from the transitions occurring from exactly one color exchange between two neighboring sites. In the case of the bipartite $SU(4)$ square lattice, the state AB can decay into four different states (AC, DA, BC, BD) when exchanging one color with the neighboring state CD , yielding four dispersive branches. However, going from AB to CD requires the exchange of two colors at least, resulting in a flat band in the harmonic order with an energy sitting at $2Jz$, i.e., the energy cost of exchanging two colors with z possible nearest neighbors.

In general, we can have bands with energy $nzJn_c$ ($n \in \{2, \dots, m\}$) depending on the number of the required color exchanges for a possible target state. Consequently, it is possible to deduce the diagonalized quadratic Hamiltonian by determining the number of color exchanges that are needed for every possible transition. In general, for any m with $k = 2$ for the square or $k = 3$ for the triangular lattice, the quadratic Hamiltonian is given by

$$\mathcal{H}^{(2)} = Jn_c \sum_{\mathbf{k}} \left\{ \sum_{n=2}^m nz \sum_{\alpha=1}^{\binom{m}{n} \binom{N-m}{n}} b_{\alpha}^{\dagger}(\mathbf{k})b_{\alpha}(\mathbf{k}) + \omega_{\text{sq/tri}}(\mathbf{k}) \sum_{\beta=1}^{m(N-m)} \left(\tilde{b}_{\beta}^{\dagger}(\mathbf{k})\tilde{b}_{\beta}(\mathbf{k}) + \frac{1}{2} \right) \right\} - \frac{m(N-m)}{2} zJn_c N, \quad (40)$$

where the sum runs over the structural Brillouin zone,

and z is the coordination number between two sublattices.

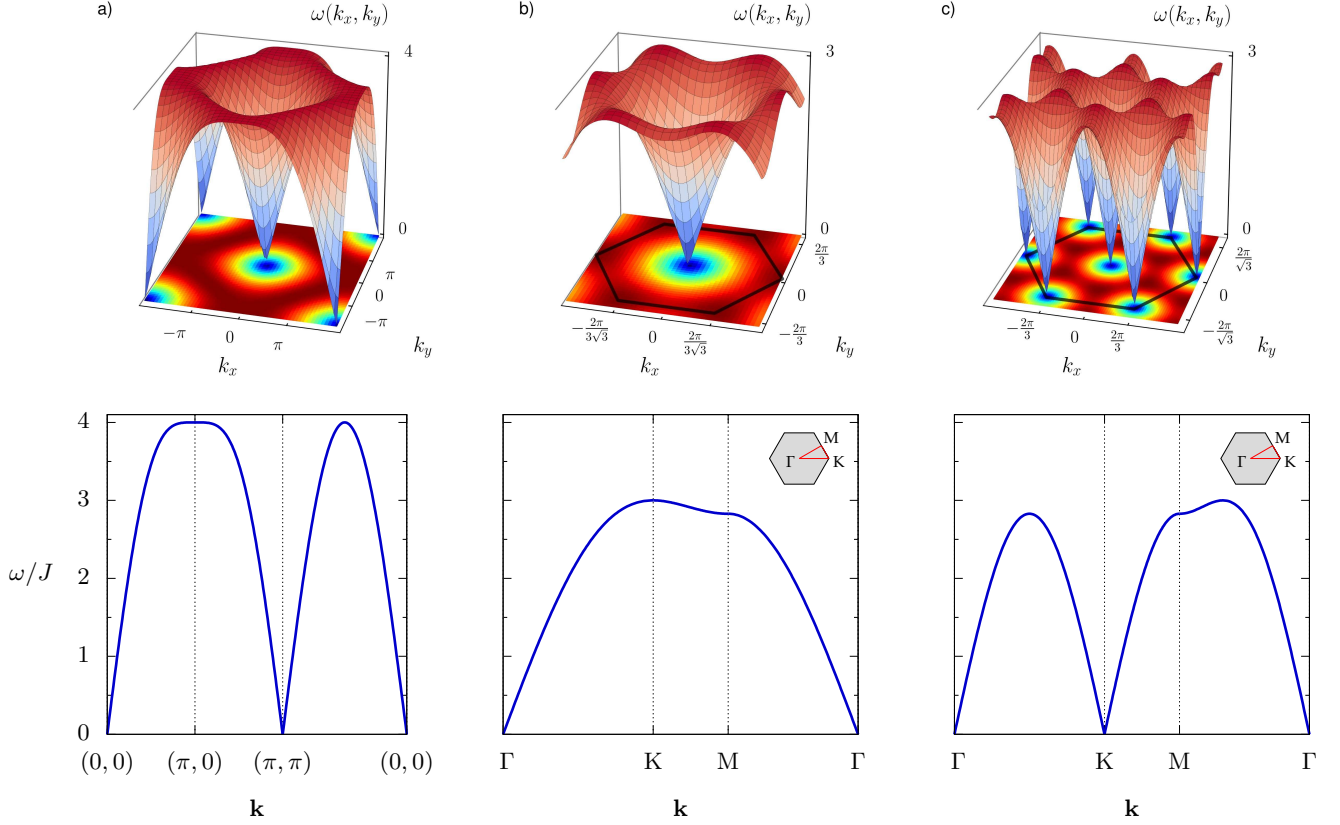


FIG. 3. The dispersion relation of the (a) SU(4) square, (b) SU(4) honeycomb, and (c) SU(6) triangular lattice. The first structural Brillouin zone is depicted in the 2D heat map. Both the honeycomb and the triangular lattices result in the identical first Brillouin zone up to a scaling factor, as the bonds between two given sublattices are identical in both lattices up to a scaling factor between the bonds.

tices ($z = 4$ for the square lattice and $z = 3$ for the triangular lattice). The dimension of the considered antisymmetric irrep $[m, 0, \dots]$ is $\binom{N}{m}$. The use of the Holstein-Primakoff bosons with the limit $n_c \rightarrow \infty$ leads to $\binom{N}{m} - 1$ branches in the structural Brillouin zone, of which $\binom{m}{1} \binom{N-m}{1} = m(N-m)$ branches are dispersive. Since $N = mn_{\text{sub}}$ for a given value of m , the square lattice will have m^2 dispersive branches and the triangular lattice will have $2m^2$ branches. Hence, we can conclude that for a given number of particles per site m , the reduction of the magnetization Δm_i is given by

$$\begin{aligned} \Delta m_i^{\text{sq}}(m) &= m^2 \left\langle \frac{1}{2} \left(\frac{4Jn_c}{Jn_c \omega_{\text{sq}}} - 1 \right) \right\rangle \\ &= 0.197m^2 \end{aligned}$$

for the square lattice, and

$$\begin{aligned} \Delta m_i^{\text{tri}}(m) &= 2m^2 \left\langle \frac{1}{2} \left(\frac{3Jn_c}{Jn_c \omega_{\text{tri}}(\mathbf{k})} - 1 \right) \right\rangle \\ &= 0.516m^2 \end{aligned}$$

for the triangular lattice.

As for the flat modes, there are $\binom{m}{n} \binom{N-m}{n}$ flat branches at energy $nzJn_c$, with $n \in \{2, \dots, m\}$ being the number of color-exchange applied at a state.

The same conclusion also applies for the honeycomb lattice, with the only difference being the number of branches that is doubled in the first structural Brillouin zone. Introducing an index ξ to account for the doubling of the branches, we obtain

$$\mathcal{H}^{(2)} = Jn_c \sum_{\mathbf{k}} \sum_{\xi=1}^2 \left\{ \sum_{n=2}^m nz \sum_{\alpha=1}^{\binom{m}{n} \binom{N-m}{n}} b_{\alpha,\xi}^\dagger(\mathbf{k}) b_{\alpha,\xi}(\mathbf{k}) + \omega_{\text{hon}}(\mathbf{k}) \sum_{\beta=1}^{m(N-m)} \left(\tilde{b}_{\beta,\xi}^\dagger(\mathbf{k}) \tilde{b}_{\beta,\xi}(\mathbf{k}) + \frac{1}{2} \right) \right\} - \frac{m(N-m)}{2} z J n_c N \quad (41)$$

for the honeycomb lattice, where $z = 3$. Hence, the reduction of the magnetization as a function of the number of particles per site is given by

$$\Delta m_i^{\text{hon}}(m) = m^2 \left\langle \frac{1}{2} \left(\frac{4Jn_c}{Jn_c \omega_{\text{hon}}(\mathbf{k})} - 1 \right) \right\rangle = 0.258m^2.$$

In all cases, the reduction of the local order parameter is much larger than 1 for $m \geq 3$, making the presence of long-range order very unlikely.

III. READ AND SACHDEV BOSONIC REPRESENTATION

Harmonic fluctuations can be analyzed with an alternative approach by using a different bosonic representation for the $SU(N)$ generators. This bosonic representation briefly mentioned in Ref. 23 is an extension of the Schwinger bosons, and can be applied to any irreps whose Young tableaux contain m rows and n_c columns. It assumes one boson for each color as well as for each row of the Young tableau, and the bosons are then antisymmetrized in accordance with the chosen irrep. In this realization, the $SU(N)$ operators can be written as

$$\hat{S}_\nu^\mu = \sum_{a=1}^m b_{\nu a}^\dagger b_{\mu a} - \frac{n_c}{2} \delta_{\mu\nu}, \quad (42)$$

where $\mu, \nu \in \{A, B, \dots\} \equiv \{1, \dots, N\}$ are the color indices and $a \in \{1, \dots, m\}$ are the row indices. They naturally satisfy the $SU(N)$ commutation relations. The constraints

$$\sum_{\alpha=1}^N b_{\alpha a}^\dagger b_{\alpha b} = \delta_{ab} n_c, \quad (43)$$

with $a \in \{1, \dots, N\}$ and $a, b \in \{1, \dots, m\}$ ensure that we work in the given irrep. The constraints that involve the same line indices are the same as the constraints of the Schwinger bosons, whereas the other equations are additional constraints that enforce the antisymmetry of the irrep.

The Heisenberg Hamiltonian in this bosonic representation is given by

$$\begin{aligned} \mathcal{H} &= J \sum_{\langle i,j \rangle} \sum_{\mu,\nu} \hat{S}_\nu^\mu(i) \hat{S}_\mu^\nu(j) \\ &= J \sum_{\langle i,j \rangle} \sum_{\mu,\nu} \sum_{a,b=1}^m b_{\nu a}^\dagger(i) b_{\mu a}(i) b_{\mu b}^\dagger(j) b_{\nu b}(j). \end{aligned} \quad (44)$$

A. $SU(4)$ $m = 2$ on the square lattice

We now turn our attention to the square lattice with $m = 2$. Let us assume an ordered state in which the colors A and B sit on the sublattice Λ_{AB} and the colors C and D are on the sublattice Λ_{CD} of the square lattice. Note that we have deliberately broken the symmetry by choosing specific colors for the sublattice. In the limit $n_c \rightarrow \infty$, we assume that there is a condensate of colors A and B on the site i and a condensate of colors C and D on the site j . Consequently, it is possible to perform the Bogoliubov substitution of the condensed bosons with c -numbers (with $c \in \mathbb{C}$), i.e.,

$$\begin{aligned} b_{Aa}^\dagger(i) &\rightarrow z_{Aa}^*, & b_{Ba}^\dagger(i) &\rightarrow z_{Ba}^*, \\ b_{Ca}^\dagger(j) &\rightarrow z_{Ca}^*, & b_{Da}^\dagger(j) &\rightarrow z_{Da}^*, \end{aligned} \quad (45)$$

for any $i \in \Lambda_{AB}$, $j \in \Lambda_{CD}$, and $a \in \{1, \dots, m\}$. This replacement is true when considering the expectation value of the bosonic number operators and the operators S_ν^μ . It is also worthwhile noting that the conventional $SU(2)$ spin-wave theory in the harmonic order also corresponds to replacing the condensed bosons by a c -number.

In this limit of the large condensate $n_c \rightarrow \infty$, the constraints (43) for the sublattice Λ_{AB} to order $\mathcal{O}(n_c)$ are reduced to

$$\begin{cases} z_{A1}^* z_{A1} + z_{B1}^* z_{B1} = n_c \\ z_{A2}^* z_{A2} + z_{B2}^* z_{B2} = n_c \\ z_{A1}^* z_{A2} + z_{B1}^* z_{B2} = 0. \end{cases} \quad (46)$$

The complex-conjugate counterpart of the third equation in Eq. (46) has been dropped as they are equivalent.

When written in a matrix form U^{AB} such that

$$z_{\mu a} =: \sqrt{n_c} [U^{AB}]_{\mu a} \quad (47)$$

with $\mu \in \{A, B\}$ (the first $\frac{N}{2}$ colors) and $a \in \{1, 2\} \equiv \{1, \dots, m\}$, the set of equations Eq. (46) amounts to imposing a unitarity condition on the matrix U^{AB} . Alternatively, the matrix elements of this unitary matrix can be parametrized in the following way. The set of equations Eq. (43) can be written as

$$\begin{cases} \sum_{a,b} z_{Aa}^* \delta_{a,b} z_{Ab} + \sum_{a,b} z_{Ba}^* \delta_{a,b} z_{Bb} = 2n_c, \\ \sum_{a,b} z_{Aa}^* \sigma_{a,b}^{(\alpha)} z_{Ab} + \sum_{a,b} z_{Ba}^* \sigma_{a,b}^{(\alpha)} z_{Bb} = 0, \end{cases} \quad (48)$$

where $\sigma_{a,b}^{(\alpha)}$ are Pauli matrices with $\alpha = x, y, z$ or

$$\begin{cases} \mathbf{z}_A^* \cdot \mathbf{z}_A + \mathbf{z}_B^* \cdot \mathbf{z}_B = 2n_c, \\ \mathbf{z}_A^* \cdot \sigma^{(\alpha)} \cdot \mathbf{z}_A + \mathbf{z}_B^* \cdot \sigma^{(\alpha)} \cdot \mathbf{z}_B = 0. \end{cases} \quad (49)$$

We can think of the problem as having two antiferromagnetically alligned SU(2) spins (the A and the B), the (z_{A1}^*, z_{A2}^*) and (z_{B1}^*, z_{B2}^*) being the SU(2) spinors of the two spins, and they can be parametrized as

$$\begin{aligned} z_{A1} &= \sqrt{n_c} e^{i\chi_{AB}} \cos \frac{\vartheta_{AB}}{2}, \\ z_{A2} &= \sqrt{n_c} e^{i\chi_{AB}} \sin \frac{\vartheta_{AB}}{2} e^{-i\varphi_{AB}}, \\ z_{B1} &= \sqrt{n_c} \sin \frac{\vartheta_{AB}}{2}, \\ z_{B2} &= -\sqrt{n_c} \cos \frac{\vartheta_{AB}}{2} e^{-i\varphi_{AB}} \end{aligned} \quad (50)$$

when condensed.

The same consideration can be done for the sublattice Λ_{CD} , starting from the constraints Eq. (43) in the limit of the large n_c :

$$\begin{cases} z_{C1}^* z_{C1} + z_{D1}^* z_{D1} = n_c \\ z_{C2}^* z_{C2} + z_{D2}^* z_{D2} = n_c \\ z_{C1}^* z_{C2} + z_{D1}^* z_{D2} = 0. \end{cases} \quad (51)$$

This can be rewritten further in a unitary matrix form U^{CD} :

$$z_{\mu a} =: \sqrt{n_c} [U^{CD}]_{\mu a} \quad (52)$$

with $\mu \in \{C, D\}$ (the last $\frac{N}{2}$ colors) and $a \in \{1, 2\} \equiv \{1, \dots, m\}$, or alternatively, with the following parametrization:

$$\begin{aligned} z_{C1} &= \sqrt{n_c} e^{i\chi_{CD}} \cos \frac{\vartheta_{CD}}{2}, \\ z_{C2} &= \sqrt{n_c} e^{i\chi_{CD}} \sin \frac{\vartheta_{CD}}{2} e^{-i\varphi_{CD}}, \\ z_{D1} &= \sqrt{n_c} \sin \frac{\vartheta_{CD}}{2}, \\ z_{D2} &= -\sqrt{n_c} \cos \frac{\vartheta_{CD}}{2} e^{-i\varphi_{CD}}. \end{aligned} \quad (53)$$

Following this procedure, the bosons $b_{Aa}^{(\dagger)}(i)$, $b_{Ba}^{(\dagger)}(i)$, $b_{Ca}^{(\dagger)}(j)$, $b_{Da}^{(\dagger)}(j)$ can be finally replaced by their corresponding c -numbers in the Hamiltonian Eq. (44), yielding a quadratic Hamiltonian $\mathcal{H}^{(2)}$ of the order $\mathcal{O}(n_c)$. After Fourier-transforming,

$$b_{\mu a}(i) = \sqrt{\frac{2}{N_{\text{sites}}}} \sum_{\mathbf{k} \in \text{RBZ}} b_{\mu a}(\mathbf{k}) \quad (54)$$

with N_{sites} being the number of sites, the quadratic Hamiltonian suited for the generalized Bogoliubov transformation is then given by

$$\mathcal{H}^{(2)} = \frac{zJn_c}{2} \sum_{\mathbf{k} \in \text{RBZ}} \left(\mathbf{b}_{\mathbf{k}}^\dagger, \mathbf{b}_{-\mathbf{k}} \right) M_{\mathbf{k}} \begin{pmatrix} \mathbf{b}_{\mathbf{k}} \\ \mathbf{b}_{-\mathbf{k}}^\dagger \end{pmatrix} - 2zJn_c N, \quad (55)$$

with $z = 4$ the coordination number and

$$\mathbf{b}_{\mathbf{k}}^\dagger = \left(b_{C1}^\dagger(\mathbf{k}), b_{C2}^\dagger(\mathbf{k}), b_{D1}^\dagger(\mathbf{k}), b_{D2}^\dagger(\mathbf{k}), \right. \\ \left. b_{A1}^\dagger(\mathbf{k}), b_{A2}^\dagger(\mathbf{k}), b_{B1}^\dagger(\mathbf{k}), b_{B2}^\dagger(\mathbf{k}) \right), \quad (56a)$$

$$\mathbf{b}_{-\mathbf{k}} = \begin{pmatrix} b_{C1}(-\mathbf{k}), b_{C2}(-\mathbf{k}), b_{D1}(-\mathbf{k}), b_{D2}(-\mathbf{k}), \\ b_{A1}(-\mathbf{k}), b_{A2}(-\mathbf{k}), b_{B1}(-\mathbf{k}), b_{B2}(-\mathbf{k}) \end{pmatrix}, \quad (56b)$$

$$M_{\mathbf{k}} = \frac{1}{2} \begin{pmatrix} \mathbb{1}_8 & B_{\mathbf{k}} \\ B_{\mathbf{k}}^\dagger & \mathbb{1}_8 \end{pmatrix}, \quad (56c)$$

$$B_{\mathbf{k}} = \begin{pmatrix} 0 & \gamma_{\mathbf{k}}^* U^\top \\ \gamma_{\mathbf{k}} U & 0 \end{pmatrix}. \quad (56d)$$

The geometrical factor $\gamma_{\mathbf{k}}$ is defined in Eq. (18) with the property that $\gamma_{-\mathbf{k}} = \gamma_{\mathbf{k}}^*$, and the matrix U stems from U_{AB} and U_{CD} :

$$U = \begin{pmatrix} z_{A1}z_{C1} & z_{A2}z_{C1} & z_{A1}z_{D1} & z_{A2}z_{D1} \\ z_{A1}z_{C2} & z_{A2}z_{C2} & z_{A1}z_{D2} & z_{A2}z_{D2} \\ z_{B1}z_{C1} & z_{B2}z_{C1} & z_{B1}z_{D1} & z_{B2}z_{D1} \\ z_{B1}z_{C2} & z_{B2}z_{C2} & z_{B1}z_{D2} & z_{B2}z_{D2} \end{pmatrix} \quad (57)$$

i.e., it is equal to $U_{AB} \otimes U_{CD}^\top$ with permuted columns, and is thus also unitary. Note that the structure of the matrix $M_{\mathbf{k}}$ above is true in general for any N and corresponding m for any of the three lattices considered in this work, as this is a consequence of the structure of the Hamiltonian in Eq. (55).

Using the matrix Y ,

$$Y = \begin{pmatrix} \mathbb{1}_8 & 0 \\ 0 & -\mathbb{1}_8 \end{pmatrix}, \quad (58)$$

the generalized Bogoliubov transformation reduces to searching the eigenvalues $\lambda \rightarrow \frac{1}{2}\omega_{\mathbf{k}}$ of the matrix $Y M_{\mathbf{k}}$. The eigenvalues can be easily found thanks to the simple block structure of this matrix. With the identity that

$$B_{\mathbf{k}}^\dagger B_{\mathbf{k}} = \begin{pmatrix} |\gamma_{\mathbf{k}}|^2 \mathbb{1}_8 & 0 \\ 0 & |\gamma_{\mathbf{k}}|^2 \mathbb{1}_8 \end{pmatrix} \quad (59)$$

for any unitary matrix U , it results that

$$Y M_{\mathbf{k}} Y M_{\mathbf{k}} = \frac{1}{4} \left(1 - |\gamma_{\mathbf{k}}|^2 \right) \mathbb{1}_{16} \\ = \lambda^2 \mathbb{1}_{16}. \quad (60)$$

The eigenvalues are then given by

$$\lambda = \pm \frac{1}{2} \sqrt{1 - |\gamma_{\mathbf{k}}|^2}. \quad (61)$$

By compactifying the notation, we finally find the diagonalized quadratic Hamiltonian

$$\mathcal{H}^{(2)} = Jn_c \sum_{\mathbf{k} \in \text{RBZ}} \omega(\mathbf{k}) \sum_{\mu=1}^8 \left(\tilde{b}_{\mu}^\dagger(\mathbf{k}) \tilde{b}_{\mu}(\mathbf{k}) + \frac{1}{2} \right) - 2zJn_c N, \quad (62)$$

in which the dispersion relation is given by

$$\omega(\mathbf{k}) = z\sqrt{1 - |\gamma_{\mathbf{k}}|^2}. \quad (63)$$

This yields the same dispersive branches as in the previous calculations in Sec. II A without the flat branches.

The different choices of the set of parameters $\vartheta_{AB}, \varphi_{AB}, \chi_{AB}$ or $\vartheta_{CD}, \varphi_{CD}, \chi_{CD}$ are all related by unitary transformations, hence they result in a unitary transformation of the matrix U in Eq. (56d). However, since Eq. (59) holds for any unitary matrix U , it follows that any unitary transformation on U leaves the eigenvalues of $M_{\mathbf{k}}$ invariant, i.e., any solution that satisfies the modified constraints Eq. (46) leads to the same dispersion relation in Eq. (63) after the Bogoliubov transformation. Thus, there exists a gauge degree of freedom $U(m)$ for each sublattice.

As an example, the solution

$$\begin{aligned} b_{A1}^\dagger(i), b_{C1}^\dagger(j) &\rightarrow \sqrt{\frac{n_c}{2}}, & b_{B1}^\dagger(i), b_{D1}^\dagger(j) &\rightarrow \sqrt{\frac{n_c}{2}}, \\ b_{A2}^\dagger(i), b_{C2}^\dagger(j) &\rightarrow -\sqrt{\frac{n_c}{2}}, & b_{B2}^\dagger(i), b_{D2}^\dagger(j) &\rightarrow \sqrt{\frac{n_c}{2}}, \end{aligned} \quad (64)$$

yields the following matrix $\tilde{B}_{\mathbf{k}}$ in Eq. (56d):

$$\tilde{B}_{\mathbf{k}} = \frac{\gamma_{\mathbf{k}}}{2} \begin{pmatrix} 1 & -1 & 1 & -1 \\ -1 & 1 & 1 & -1 \\ 1 & 1 & 1 & 1 \\ -1 & -1 & 1 & 1 \end{pmatrix}, \quad (65)$$

which in turn results in the dispersion relation (63) after the Bogoliubov transformation.

B. Arbitrary m on different lattices

The analysis in Sec. III A can be straightforwardly generalized to any N and m for a two-sublattice order, i.e., on the square or honeycomb lattice. This is also easily applied to the three-sublattice order on the triangular lattice. The only difference with the two-sublattice order is in the Hamiltonian generated after the c -number replacement of the condensed bosons. Unlike in the two-sublattice order calculations where the resulting Hamiltonian is purely quadratic, higher-order terms are generated in the Hamiltonian, i.e.,

$$\mathcal{H} = \mathcal{H}^{(2)} + \mathcal{H}^{(3)} + \mathcal{H}^{(4)}, \quad (66)$$

where $\mathcal{H}^{(2)} \propto \mathcal{O}(n_c)$, $\mathcal{H}^{(1)} \propto \mathcal{O}(n_c^{\frac{1}{2}})$ and $\mathcal{H}^{(1)} \propto \mathcal{O}(1)$. However, once we truncate the Hamiltonian to keep only the dominant term of the order $\mathcal{O}(n_c)$, the rest of the calculations are identical to Sec. III A. Hence, the procedure can be applied to any of the three lattice geometries considered in this work. For given N , m and assuming a color-ordered ground-state on one of the three lattices

we considered, let us denote the color index of one of the condensed colors on each sublattice $l \in \{1, \dots, k\}$ by $\mu^l \in \{1, \dots, m\}$, and $a, b \in \{1, \dots, m\}$. In the limit $n_c \rightarrow \infty$, this allows one to use the Bogoliubov prescription of replacing the bosons by a c -number, provided that the numbers satisfy the antisymmetrization constraints (43). In the large- n_c limit, these constraints become

$$\sum_{\mu^l=1}^m z_{\mu a}^{l*} z_{\mu b}^l = \delta_{ab} n_c. \quad (67)$$

for each sublattice i with corresponding condensed boson colors μ . One particular solution that satisfies the constraints Eq. (67) are

$$z_{\mu a}^l \rightarrow \varphi_{\mu a}^l(m) \sqrt{\frac{n_c}{m}} := \sqrt{n_c} U_{\mu a}^l, \quad (68)$$

with the phase $\varphi_{\mu a}^l(m)$ defined by

$$\varphi_{\mu a}^l(m) := e^{-i(a-1)\frac{2\pi}{m}\mu}. \quad (69)$$

It can be easily verified that $z_{\mu a}$ satisfies the constraints by using the identity $\sum_{k=0}^{n-1} e^{q\frac{2\pi i}{n}k} = 0$, where $n \in \mathbb{N}_{>2}$ and $q \in \{1, \dots, n-1\}$. An example of the phases for four condensed bosons per site ($m=4$) for SU(8) on the square/honeycomb lattice or for SU(12) on the triangular lattice is shown in Table I. Any unitary transformation on the matrix U^l yields a solution of Eq. (67).

| $\mu \in \{A, B, C, D\}$ | $a=1$ | $a=2$ | $a=3$ | $a=4$ |
|--------------------------|-------|------------|------------|-------------|
| A | 0 | e^{-ix} | e^{-2ix} | e^{-3ix} |
| B | 0 | e^{-2ix} | e^{-4ix} | e^{-6ix} |
| C | 0 | e^{-3ix} | e^{-6ix} | e^{-9ix} |
| D | 0 | e^{-4ix} | e^{-8ix} | e^{-12ix} |

TABLE I. Phases $\varphi_{\mu a}(m)$ of the numbers replacing the condensed bosons that satisfy the antisymmetry constraints for $m=4$. The phase $\varphi_{\mu a}$ for a given μ and a can be read from the Table, in which $x := \frac{2\pi}{m}$.

Note that it is also possible to parametrize the bosons similarly to Eq. (50) and Eq. (53) by using the generalized Gell-Mann matrices in Eq. (48) that is adapted to N and m .

Out of the Nm bosons per site, $\frac{N}{n_{\text{sub}}}m = m^2$ bosons are replaced by complex numbers satisfying the antisymmetrization constraints. The Bogoliubov transformation can then be performed to diagonalize the quadratic Hamiltonian, yielding $Nm - m^2 = m(N - m)$ branches in the structural Brillouin zone. The resulting dispersive branches and the number of these branches are identical to the results obtained with the multibosonic approach in Sec. IID without the flat branches. Hence the same conclusion regarding the ordered color-moment can be drawn, namely that the only Heisenberg system that can potentially retain the color-ordered ground-state is the SU(4) particles with $m=2$ on the square lattice.

IV. DISCUSSION

As seen in the previous considerations in the harmonic order, the flat branches we obtained with the multi-bosonic method are related to the multipole moments requiring more than one ladder-operator action. Since the Heisenberg Hamiltonian contains the bilinear term only, these transitions will thus result in localized branches in the quadratic order, and they do not intervene in the reduction of the ordering. The reduction of the color order originates solely from the fluctuations that come from the permitted decay channels that yield the dispersive branches.

The multiboson spin wave in SU(2) spin- S systems as in Ref. 35 gives us an insight to this method. When applied to a SU(2) Heisenberg spin- S systems to the harmonic order, $2S$ branches emerge in the structural Brillouin zone from which one branch is dispersive and the rest are flat. The dispersive branch describes the dipole moments of the spins on neighboring sites, i.e., one spin flip that results in the reduction of the fully polarized state $S_{\max} = \pm S$ by one quantum $\Delta S_z = \mp 1/2$. The flat branches correspond to the higher-order transitions requiring more than one spin-flip, thus reducing the polarization by more than one quantum. It turns out that the dispersive branch is identical to the dispersive relation one obtains with the conventional spin-wave theory for spin S (but in the fundamental irrep), and one obtains exactly one band. In contrast, higher SU(N) symmetries yield more than one dispersive branch due to the more intricate group structure. For $N > 2$, there are more possible ways to change a color, i.e., there are $N(N-1)/2$ pairs of ladder operators (\hat{S}_ν^μ , $\mu \neq \nu$) whereas SU(2) possesses only one pair of ladder-operators.

The accessible states by one color exchange can be schematically represented with the weight diagram of the corresponding irrep, in which a state is associated to a point [an example of a weight diagram for the SU(4) $[0,1,0]$ irrep is shown in Figure 4]. For a given state, the states that can be reached by one color exchange are the adjacent points on the weight diagram. The edges that connect points are in one of the $N(N-1)/2$ directions that represent the action of the ladder operators \hat{S}_ν^μ , $\mu \neq \nu$, and each direction is associated to one specific color exchange. In our example, it can be seen that the a state in the irrep \square of SU(4) has four adjacent points, thus showing the four states accessible by one color permutation. The action of the ladder operators of SU(N) can be depicted as the $N(N-1)/2$ directions in which the vertices between each point lie.

The Hamiltonian obtained through this method that describes the dynamics of these quantum fluctuations yields the same dispersive branches as in the second method with Read and Sachdev bosons in Sec. III, although the bosonic representations are different in both cases. The second approach has the advantage of containing exclusively the physical branches at the quadratic order which contribute to the quantum fluctuations —

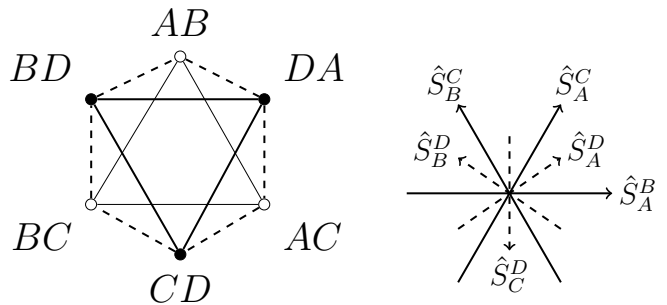


FIG. 4. Left panel: weight diagram of SU(4) in the anti-symmetric $m = 2$ irrep. The group SU(4) being a group of rank 3, the states are characterized by three coordinates and the weight diagram is thus in 3D. The dots and the circles compose two different planes, the dots being on top of the circles. Right panel: the direction in which the six SU(2) ladder-operators (\hat{S}_ν^μ , $\mu \neq \nu$) operate. The dotted lines have a non-zero component in the normal of the plane. One can attribute the labels A, B, C, D to the states accordingly.

the flat multipolar branches do not appear. Apart from these silent modes, they both give rise to the same results and yield identical values of the ordered moment for each system we investigated.

According to the preceding analysis of the magnetization in Section II, the color order persists in the bipartite square lattice with two SU(4) particles per site, but it is destroyed in the bipartite honeycomb lattice, although the considered symmetry is identical (SU(4)) in both bipartite lattices. This behavior is also observed in the SU(2) spin- $\frac{1}{2}$ AFM Heisenberg model. Comparing the values of the magnetization taken from Ref. 39 and Ref. 40, we observe that the magnetization is smaller on the Néel honeycomb lattice than on the Néel square lattice. The smaller coordination number z of the honeycomb lattice leads to stronger quantum fluctuations, thus destroying the magnetic order. It is worthwhile noting that the ratio of the reduction of the magnetic moment between the square lattice and the honeycomb lattice $0.1966/0.2582 = 0.7614$ is the same as that of the reduction of the color moment of our models, $0.7864/1.0328 = 0.7614$.

The tripartite triangular lattice with two SU(6) particles per site also does not retain a finite color order. However, the difference with the bipartite square lattice comes from the higher symmetry of SU(6) in this case. As N grows, the number of decay channels of the quantum fluctuations becomes also larger. Hence, the quantum fluctuations are stronger, and order is not favored as a consequence. As the study above involved the smallest non-trivial $m = N/k$ possible for each geometry, we expect that the only possible candidate for the color order with many particles per site is the SU(4) Heisenberg model on the bipartite square lattice. A pinning-field QMC study on this model has shown that this model retains a finite magnetization of $m_i^{\text{alt}} \approx 0.24 - 0.26$ at their largest system size and largest U ,¹⁴ a value similar to

our result in Eq. (28). However, a different QMC study shows results with no apparent broken lattice symmetry.¹⁰ Hence, these results call upon further investigation to settle the existence or non-existence of the magnetic order on this model.

V. CONCLUSION

We have applied the LFWT to systems with more than one particle per site described by fully antisymmetric $SU(N)$ irreducible representations that are relevant to experiments with optical traps with more than one particle per site, first in the spirit of the multiboson spin-wave theory and secondly using a different bosonic representation for antisymmetric $SU(N)$ irreps. Both methods allow one to compute the ordered moment of the system and produce identical results. They predict that the $SU(4)$ AFM Heisenberg model on the bipartite square lattice with two particles ($m = 2$) retains a finite long-range order even after including quantum fluctuations within the realm of the LFWT. The suggestion that this system could be magnetically ordered allows one to po-

tentially fill the corresponding point in the phase diagram of the $SU(N)$ square lattice in Ref. 24. However, it is likely that the quantum fluctuations destroy completely the color order for higher N with $k = 2$ as expected, due to the increase of quantum fluctuations with increasing N . This is also true for the honeycomb lattice and the triangular lattice, where the ordered moment is destroyed even for $m = 2$, the smallest permissible m assuming a two-sublattice order or a three-sublattice order, respectively. The stronger quantum fluctuations in the bipartite honeycomb lattice compared to the bipartite square lattice with the same $SU(4)$ symmetry are explained by the lower coordination number z that reinforces quantum fluctuations.

ACKNOWLEDGMENTS

We would like to thank Andrew Smerald and Miklós Lajkó for useful discussions. This work has been supported by the Swiss National Science Foundation and by the Hungarian OTKA Grant No. K106047.

-
- ¹ A. V. Gorshkov, M. Hermele, V. Gurarie, C. Xu, P. S. Julienne, J. Ye, P. Zoller, E. Demler, M. D. Lukin, and A. M. Rey, *Nature Physics* **6**, 289 (2010).
- ² F. Scazza, C. Hofrichter, M. Höfer, P. C. De Groot, I. Bloch, and S. Fölling, *Nature Physics* (2014), 10.1038/nphys3061.
- ³ X. Zhang, M. Bishof, S. L. Bromley, C. V. Kraus, M. S. Safronova, P. Zoller, A. M. Rey, and J. Ye, *science* **345**, 1467 (2014).
- ⁴ B. Sutherland, *Phys. Rev. B* **12**, 3795 (1975).
- ⁵ B. Frischmuth, F. Mila, and M. Troyer, *Phys. Rev. Lett.* **82**, 835 (1999).
- ⁶ L. Messio and F. Mila, *Phys. Rev. Lett.* **109**, 205306 (2012).
- ⁷ L. Bonnes, K. R. A. Hazzard, S. R. Manmana, A. M. Rey, and S. Wessel, *Phys. Rev. Lett.* **109**, 205305 (2012).
- ⁸ P. Nataf and F. Mila, *Physical Review B* **93** (2016), 10.1103/PhysRevB.93.155134.
- ⁹ P. Nataf and F. Mila, *Physical Review Letters* **113** (2014), 10.1103/PhysRevLett.113.127204.
- ¹⁰ F. F. Assaad, *Physical Review B* **71** (2005), 10.1103/PhysRevB.71.075103.
- ¹¹ K. S. D. Beach, F. Alet, M. Mambrini, and S. Capponi, *Phys. Rev. B* **80**, 184401 (2009).
- ¹² Z. Cai, H.-H. Hung, L. Wang, and C. Wu, *Phys. Rev. B* **88**, 125108 (2013).
- ¹³ T. C. Lang, Z. Y. Meng, A. Muramatsu, S. Wessel, and F. F. Assaad, *Phys. Rev. Lett.* **111**, 066401 (2013).
- ¹⁴ D. Wang, Y. Li, Z. Cai, Z. Zhou, Y. Wang, and C. Wu, *Phys. Rev. Lett.* **112**, 156403 (2014).
- ¹⁵ A. Paramekanti and J. B. Marston, *J. Phys.: Condens. Matter* **19**, 125215 (2007).
- ¹⁶ F. Wang and A. Vishwanath, *Phys. Rev. B* **80**, 064413 (2009).
- ¹⁷ M. Lajkó and K. Penc, *Phys. Rev. B* **87**, 224428 (2013).
- ¹⁸ J. Dufour, P. Nataf, and F. Mila, *Physical Review B* **91** (2015), 10.1103/PhysRevB.91.174427.
- ¹⁹ J. Dufour and F. Mila, *Phys. Rev. A* **94**, 033617 (2016).
- ²⁰ P. Corboz, A. M. Läuchli, K. Penc, M. Troyer, and F. Mila, *Physical Review Letters* **107** (2011), 10.1103/PhysRevLett.107.215301.
- ²¹ P. Corboz, M. Lajkó, A. M. Läuchli, K. Penc, and F. Mila, *Physical Review X* **2** (2012), 10.1103/PhysRevX.2.041013.
- ²² P. Corboz, K. Penc, F. Mila, and A. M. Läuchli, *Phys. Rev. B* **86**, 041106 (2012).
- ²³ N. Read and S. Sachdev, *Nuclear Physics B* **316**, 609 (1989).
- ²⁴ M. Hermele and V. Gurarie, *Physical Review B* **84** (2011), 10.1103/PhysRevB.84.174441.
- ²⁵ M. Hermele, V. Gurarie, and A. M. Rey, *Physical Review Letters* **103** (2009), 10.1103/PhysRevLett.103.135301.
- ²⁶ T. A. Tóth, A. M. Läuchli, F. Mila, and K. Penc, *Physical Review Letters* **105** (2010), 10.1103/PhysRevLett.105.265301.
- ²⁷ C. Luo, T. Datta, and D.-X. Yao, *Phys. Rev. B* **93**, 235148 (2016).
- ²⁸ N. Papanicolaou, *Nuclear Physics B* **240**, 281 (1984).
- ²⁹ N. Papanicolaou, *Nuclear Physics B* **305**, 367 (1988).
- ³⁰ A. Joshi, M. Ma, F. Mila, D. N. Shi, and F. C. Zhang, *Phys. Rev. B* **60**, 6584 (1999).
- ³¹ A. V. Chubukov, *J. Phys.: Condens. Matter* **2**, 1593 (1990).
- ³² H. Tsunetsugu and M. Arikawa, *J. Phys. Soc. Jpn.* **75**, 083701 (2006).
- ³³ A. Läuchli, F. Mila, and K. Penc, *Phys. Rev. Lett.* **97**, 087205 (2006).
- ³⁴ M. Masashige, K. Haruhiko, S. Tomoyuki, and M. Takatsugu, *J. Phys. Soc. Jpn.* **79**, 084703 (2010).

- ³⁵ J. Romhányi and K. Penc, *Physical Review B* **86** (2012), [10.1103/PhysRevB.86.174428](https://doi.org/10.1103/PhysRevB.86.174428).
- ³⁶ K. Penc, J. Romhányi, T. Rõm, U. Nagel, Á. Antal, T. Fehér, A. Jánossy, H. Engelkamp, H. Murakawa, Y. Tokura, D. Szaller, S. Bordács, and I. Kézsmárki, *Phys. Rev. Lett.* **108**, 257203 (2012).
- ³⁷ N. N. Bogolyubov, *J. Phys.(USSR)* **11**, 23 (1947), [*Izv. Akad. Nauk Ser. Fiz.*11,77(1947)].
- ³⁸ B. Bauer, P. Corboz, A. M. Läuchli, L. Messio, K. Penc, M. Troyer, and F. Mila, *Physical Review B* **85** (2012), [10.1103/PhysRevB.85.125116](https://doi.org/10.1103/PhysRevB.85.125116).
- ³⁹ P. W. Anderson, *Phys. Rev.* **86**, 694 (1952).
- ⁴⁰ Z. Weihong, J. Oitmaa, and C. J. Hamer, *Physical Review B* **44**, 11869 (1991).